Journal of Solid State Chemistry 184 (2011) 481–487

Contents lists available at ScienceDirect

Journal of Solid State Chemistry

journal homepage: www.elsevier.com/locate/jssc

# The C–F…F–C short contacts in the metal complexes of fluoro-phenyl-acrylic acids

Gui-lei Liu [a], Cai-Ming Liu [b], Hui Li [a,*]

[a] Key Laboratory of Cluster Science of Ministry of Education, Department of Chemistry, School of Science, Beijing Institute of Technology, Beijing 100081, PR China
[b] Institute of Chemistry, Chinese Academy of Science, Beijing 100190, PR China

ARTICLE INFO

*Article history:*
Received 17 June 2010
Received in revised form
16 December 2010
Accepted 23 December 2010
Available online 1 January 2011

*Keywords:*
Halogen–halogen interaction
Fluoro-cinnamic acid
Supramolecular chemistry
Coordination polymer
Magnetic exchange property

ABSTRACT

Four new complexes of fluoro-phenyl-acrylic acids (E)-3-(3-fluoro-phenyl)-acrylic acid (*L1*) $[Mn_3(L1)_6(L2)_2]\cdot H_2O\cdot CH_3CN$ (**1**), $[Zn_2(L1)_4(L3)]_n$ (**2**), $[Mn(L1)_2(H_2O)_2]_n$ (**3**) and $[Co(L1)_2(H_2O)_2]_n$ (**4**) (*L2*=1,10-phenanthroline, *L3*=4,4′-bipy) have been synthesized based on the molecular design and research of halogen–halogen interactions (especially fluoro–fluoro contact). The structure analyses reveal that complex **1** is a trinuclear complex, which is blocked by *L2*. Complex **2** is a 1D chain bridged through *L3*. Complexes **3** and **4** exhibit 2D grid like metal–organic framework structures through carboxylato bridge ligand. Variable-temperature magnetic measurements showed an antiferromagnetic interaction between Mn(II) ions and between Co(II) ions in complexes **3** and **4**, respectively. A short C–F…F–C contact with a distance of 2.953 Å was found between the trinuclear coordination compound **1**.



## 1. Introduction

Intermolecular interactions such as hydrogen bonding, π–π stacking interactions, van der Waals interactions and others have been studied in the self-assembly of molecules in crystal lattices [1–14]. Recently, the study of halogen–hydrogen bonding and halogen–halogen bonding in organic supramolecular systems has aroused great attention [15–17]. Halogen–halogen contacts are characterized by the fact that the interhalogen distance is less than the sum of van der Waals radii ($r_{vdW}$) of the corresponding halogen atoms [18,19]. Although the physical origin of short halogen–halogen contacts is still a controversy at present, it has been generally accepted that the short contact frequently exists between halogen atoms or between a carbon-bonded halogen atom and an electronegative atom in molecular crystals. There are two preferred arrangements for these contacts: the first arrangement occurs when $R-Y1\ldots Y2$ angle = $Y1\ldots Y2-R$ angle (type I in Scheme 1). The second arrangement occurs when the $R-Y1\ldots Y2$ angle = 180° and the $Y1\ldots Y2-R$ angle = 90° (type II in Scheme 1). Christer and Aakeroy [20] have studied a series of organic supramolecular systems containing I…I bonds and N…I bonds. Subsequently, Cincic and Jones [21] have explained the stepwise mechanism for the formation of halogen-bonded chains involving the strong N…I and weak S…I bonds. A series of C–Br…Br–C, C–Br…Br–Fe and Fe–Br…Br–Fe contacts and short C–Cl…Cl–C contacts have been reported one after another in organic supramolecular systems very recently [22,23]. Meanwhile, the influence of organic fluorine in crystal packing has been a subject of controversy. In the first instance, because fluorine is highly electronegative and of the high polarity of the C–F bond, the tendency of the C–F bond to segregate and pack separately due to less attractive C–F…F–C interactions have been reported [19,24]. However, experimental charge density and topological analysis have demonstrated that F…F intermolecular interactions are significantly detectable and reinforce the crystal packing [25–29]. To the best of our knowledge, the research reports about halogen–hydrogen bonds and halogen–halogen interactions mainly in organic compounds [30–34]. How about halogen–halogen interactions in coordination compounds rather than organic molecules? Is there any difference in the F…F interaction between coordination compound molecules and organic molecules? These questions lead us to build several novel coordination compounds including C–F…F–C units based on our research of acrylic acid coordination chemistry.

In our previous work, we have studied the transition-metal and lanthanide coordination complexes with (E)-3-(2, or 3, or 4-hydroxyl-phenyl)-acrylic acid ligand [35,36]. The OH-substitute acrylic acid usually produced the discrete mononuclear, dinuclear or one-dimensional coordination polymers, and no carboxylato-bridged 2D structure. To extend the systematic research of coordination chemistry of acrylic acid ligand, F-substitute acrylic acid has been selected to check the fluoro–fluoro contact besides

* Corresponding author. Fax: +86 10 82575113.
*E-mail address:* lihui@bit.edu.cn (H. Li).

0022-4596/$ - see front matter © 2010 Elsevier Inc. All rights reserved.
doi:10.1016/j.jssc.2010.12.022

the coordination modes of carboxylato group. Herein, we report four complexes $[Mn_3(L1)_6(L2)_2]\cdot H_2O\cdot CH_3CN$ (**1**), $[Zn_2(L1)_4(L3)]_n$ (**2**), $[Mn(L1)_2(H_2O)_2]_n$ (**3**), $[Co(L1)_2(H_2O)_2]_n$ (**4**) (*L1*=(E)-3-(3-fluoro-phenyl)-acrylic acid, *L2*=1,10-phenanthroline, *L3*=4,4′-bipy). Compound **1** is a trinuclear complex. Compound **2** is a 1D chain bridged by ligand *L3*. Compounds **3** and **4** exhibit 2D metal–organic framework structures. They are all further assembled into 3D supramolecular framework structures through non-conventional C−H…F interactions, π–π stacking interactions and F…F interactions.

## 2. Experimental

### 2.1. General remarks

The reagents and solvents used were of commercially available reagent quality unless otherwise stated. Variable-temperature magnetic susceptibility was measured on a Quantum Design MPMSXL5 (SQUID) magnetometer. Diamagnetic corrections were estimated from Pascal's constants for all constituent atoms. Elemental analyses (C, H, N) were carried out at the Beijing Institute of Technology. FT-IR spectrum is recorded in the Nicolet-360 FT-IR spectrometer.

### 2.2. Synthesis of $[Mn_3(L1)_6(L2)_2]\cdot H_2O\cdot CH_3CN$ (**1**)

A methanol solution (3 mL) of $MnCl_2\cdot 6H_2O$ (0.015 g, 0.05 mmol) was mixed with a methanol (5 mL) solution of (E)-3-(3–fluoro-phenyl)-acrylic acid (0.025 g, 0.15 mmol). 0.015 g of triethylamine was added drop-wise to this mixture to bring the pH of the solution to about 7 with constantly stirring for 30 min. Then an acetonitrile solution (3 mL) of 1,10-phenanthroline(0.015 g, 0.075 mmol) was added drop-wise to this mixture with constantly stirring by adding about 0.2 mL of DMF. The result solution was then filtered and left at room temperature. Yellow rectangular-shaped single crystals suitable for X-ray diffraction were obtained by slow evaporation for several days. Anal. Calcd. for $C_{80}H_{56}F_6Mn_3N_5O_{13}$: C, 61.19; H, 3.61; F, 7.30; N, 4.30; O, 13.06. Found: C, 61.17; H, 3.59; N, 4.34. IR (KBr pellet, $cm^{-1}$): 1644$\nu_{as}$($COO^-$), 1394$\nu_s$($COO^-$), 1345$\nu$(C=N) and1265$\nu$(C–F).

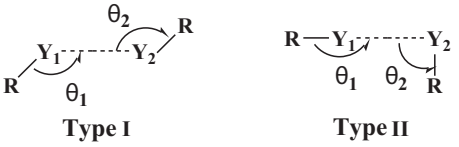


**Scheme 1.**

### 2.3. Synthesis of $[Zn_2(L1)_4(L3)]_n$ (**2**)

Compound **2** was obtained by following a similar procedure to that of **1**; $Zn(NO_3)_2\cdot 6H_2O$ and 4,4′-bipy were used in place of $MnCl_2\cdot 6H_2O$ and 1,10-phenanthroline, respectively. Colorless prism single crystals suitable for X-ray diffraction were obtained by slow evaporation of the mother liquor for several days. Anal. Calcd for $C_{46}H_{32}F_4N_2O_8Zn_2$: C, 58.31; H, 3.40; F, 8.02; N, 2.96; O, 13.51. Found: C, 58.27; H, 3.42; N, 2.97. IR (KBr pellet, $cm^{-1}$): 1649$\nu_{as}$($COO^-$), 1405$\nu_s$($COO^-$), 1311$\nu$(C=N) and 1268$\nu$(C–F).

### 2.4. Synthesis of $[Mn(L1)_2(H_2O)_2]_n$ (**3**)

A methanol solution (3 mL) of $MnCl_2\cdot 4H_2O$ (0.015 g, 0.075 mmol) was mixed with a methanol (5 mL) solution of (E)-3-(3–fluoro-phenyl)-acrylic acid (0.025 g, 0.15 mmol). 0.015 g of triethylamine was added drop-wise to this mixture to bring the pH of the solution to about 7 with constantly stirring for 30 min. The resulting solution was then filtered and left at room temperature. Yellow diamond-shaped single crystals suitable for X-ray diffraction were obtained by slow evaporation of the mother liquor for 5 days. Anal. Calcd for $C_{18}H_{16}F_2MnO_6$: C, 45.38; H, 3.38; F, 7.98; O, 20.15. Found: C, 45.36; H, 3.39. IR (KBr pellet, $cm^{-1}$): 1640$\nu_{as}$($COO^-$), 1411$\nu_s$($COO^-$) and 1268$\nu$(C–F).

**Table 1**
Crystal data and structure refinement for **1–4.**

| Complex | **1** | **2** | **3** | **4** |
|---|---|---|---|---|
| Formula | $C_{80}H_{56}F_6N_5O_{13}Mn_3$ | $C_{28}H_{20}F_2N_2O_4Zn$ | $C_{18}H_{16}F_2MnO_6$ | $C_{18}H_{16}CoF_2O_6$ |
| M ($mol^{-1}$) | 1562.04 | 551.83 | 476.24 | 484.24 |
| $T$ (K) | 93(2) | 293(2) | 293(2) | 88(2) |
| $\lambda$(Mo$K\alpha$) (Å) | 0.71073 | 0.71073 | 0.71073 | 0.71073 |
| Crystal system | Triclinic | Triclinic | Monoclinic | Monoclinic |
| Space group | $P$–1 | $P$–1 | $P2_1/c$ (14) | $P2_1/c$ (14) |
| $a$ (Å) | 11.436(2) | 7.8034(13) | 18.9066(13) | 18.73 (2) |
| $b$ (Å) | 12.420(3) | 10.1748(15) | 6.4578(5) | 6.391(8) |
| $c$ (Å) | 13.799(3) | 13.169(2) | 7.4479(5) | 7.348(9) |
| $\alpha$ (deg) | 109.695(2) | 77.289(4) | 90.00 | 90.00 |
| $\beta$ (deg) | 98.3920(10) | 89.780(5) | 94.40 | 93.29 |
| $\gamma$ (deg) | 100.020(2) | 77.660(4) | 90.00 | 90.00 |
| $V$ ($Å^3$) | 1772.3(6) | 995.4(3) | 906.67(30) | 877.9(19) |
| $Z$ | 1 | 2 | 1 | 2 |
| $\rho$(calculated) (g $cm^{-3}$) | 1.464 | 1.581 | 1.31033 | 1.609 |
| $\mu$(Mo$K\alpha$) ($mm^{-1}$) | 0.611 | 1.299 | 0.432 | 1.031 |
| $F$(0 0 0) | 798 | 564 | 365 | 434 |
| $\theta$ Range (deg) | 3.04–26.50 | 3.02–27.49 | 3.24–27.86 | 3.27–26.50 |
| $R1$, $I>2\sigma(I)$ (all) | 0.0614 | 0.0456 | 0.0494 | 0.0638 |
| $WR_2$, $I>2\sigma(I)$ (all) | 0.1241 | 0.1162 | 0.1422 | 0.1548 |
| Total reflections | 13,135 | 8191 | 5234 | 6057 |
| Unique data ($R_{int}$) | 7101 (0.0246) | 6202 (0.0219) | 2085 (0.0360) | 1773 (0.0809) |
| $S$(GOF) | 0.993 | 1.013 | 1.066 | 1.009 |
| $\Delta\rho_{max,\ min}$ (e $Å^{-3}$) | 1.189, −0.584 | 2.527, −0.506 | 0.772, −0.458 | 0.9374, −0.928 |

### 2.5. Synthesis of $[Co(L1)_2(H_2O)_2]_n$ (**4**)

Compound **4** was obtained by following a similar procedure to that of compound **3**; $CoCl_2 \cdot 6H_2O$ was used in place of $MnCl_2 \cdot 4H_2O$. Pink diamond-shaped transparent single crystals suitable for X-ray diffraction were obtained after a few days of storage of the filtrate. Anal. Calcd for $C_{18}H_{16}CoF_2O_6$: C, 44.63; H, 3.33; F, 7.85; O, 19.82. Found: C, 44.67; H, 3.31. IR (KBr pellet, $cm^{-1}$): 1640$\nu_{as}$($COO^-$), 1411$\nu_s$($COO^-$) and 1268$\nu$(C–F).

### 2.6. Crystal data collection and refinement

Single-crystal X-ray diffraction data were collected on a Rigaku RAXIS-RAPID CCD diffractometer equipped with a graphite-monochromatic Mo$K\alpha$ radiation ($\lambda$=0.71073 Å) using an $\omega$ scan mode at 93(2) or 293(2) K. Unit-cell parameters were determined from automatic centering of reflections and refined by least-squares method. Crystallographic data of compounds **1**–**4** are given in Table 1. Selected bond distances and angles are given in Tables 2–4. All non-hydrogen atoms were located by direct methods and subsequent difference Fourier syntheses. The hydrogen atoms bound to carbon were located by geometrical calculations, and their positions and thermal parameters were fixed during structure refinement. All non-hydrogen atoms were refined by full-matrix least-squares techniques with $I > 2\sigma(I)$. All calculations were performed by SHELXTL 97 program [37].

**Table 2**
Bond lengths (Å) and angles (deg) in the Mn(II) coordination spheres in **1.**

| | | | |
|---|---|---|---|
| Mn(1)–O(1) | 2.270(2) | Mn(1)–O(2) | 2.287(2) |
| Mn(1)–O(3) | 2.093(2) | Mn(1)–O(5) | 2.096(3) |
| Mn(1)–N(2) | 2.268(3) | Mn(2)–O(1)[a] | 2.204(2) |
| Mn(2)–O(4)[a] | 2.168(3) | Mn(2)–O(6)[a] | 2.165(3) |
| C(9)–O(1)–Mn(1) | 90.88(19) | C(9)–O(1)–Mn(2) | 132.0(2) |
| C(9)–O(2)–Mn(1) | 91.14(18) | Mn(2)–O(1)–Mn(1) | 108.71(9) |
| C(18)–O(3)–Mn(1) | 129.3(2) | C(18)–O(4)–Mn(2) | 144.3(2) |
| C(27)–O(5)–Mn(1) | 134.0(2) | C(27)–O(6)–Mn(2) | 137.8(2) |

[a] Symmetry code: $-x+1$, $-y+1$, $-z+1$.

**Table 3**
Bond lengths (Å) and angles (deg) in the Zn(II) coordination spheres in **2.**

| | | | |
|---|---|---|---|
| Zn(1)–O(1) | 2.0219(17) | Zn(1)–O(2)[a] | 2.0406(17) |
| Zn(1)–N(1) | 2.0389(19) | Zn(1)–O(4)[a] | 2.0587(17) |
| Zn(1)–O(3) | 2.2039(19) | Zn(1)–Zn(1)[a] | 2.9314(6) |
| O(1)–Zn(1)–N(1) | 99.64(8) | O(1)–Zn(1)–O(2)[a] | 160.67(7) |
| O(1)–Zn(1)–O(3) | 91.48(7) | O(1)–Zn(1)–O(4)[a] | 88.32(7) |
| N(1)–Zn(1)–O(3) | 100.13(7) | N(1)–Zn(1)–O(4)[a] | 99.22(7) |
| C(9)–O(1)–Zn(1) | 126.50(15) | C(23)–N(1)–Zn(1) | 121.51(16) |
| N(1)–Zn(1)–Zn(1)[a] | 176.20(6) | O(1)–Zn(1)–Zn(1)[a] | 81.05(5) |

[a] Symmetry code: $-x+2$, $-y+1$, $-z+1$.

**Table 4**
Bond lengths (Å) and angles (deg) in the Mn(II) coordination spheres in **3.**

| | | | |
|---|---|---|---|
| Mn(1)–O(1) | 2.1633(19) | Mn(1)–O(2) | 2.1766(19) |
| Mn(1)–O(3) | 2.2039(19) | – | – |
| O(1)[a]–Mn(1)–O(1) | 180.00(11) | O(1)–Mn(1)–O(2) | 93.72(7) |
| O(1)[a]–Mn(1)–O(2) | 86.28(7) | O(1)–Mn(1)–O(3) | 92.89(8) |
| O(1)[a]–Mn(1)–O(3) | 87.11(8) | O(2)–Mn(1)–O(3) | 96.84(8) |
| O(1)–Mn(1)–O(3)[a] | 87.11(8) | O(2)–Mn(1)–O(3)[a] | 83.16(8) |
| C(9)–O(1)–Mn(1) | 128.08(16) | C(9)[b]–O(2)–Mn(1) | 131.91(18) |

[a] Symmetry code: $-x+1$, $-y+1$, $-z$.
[b] Symmetry code: $x$, $-y+1/2$, $z-1/2$.

**Table 5**
Important observed hydrogen bonding in compounds **1**–**4** (in Å and deg).

| Complex | *D*–*H*…*A* | *d* (*H*…*A*) (Å) | *d* (*D*…*A*) (Å) | ∠*DHA* (deg) |
|---|---|---|---|---|
| **1** | F3…H5A–C5A | 2.554 | 3.391 | 147.2 |
| | F1…H35B–C35B | 2.890 | 3.812 | 164.2 |
| **2** | F1…H12B–C12A | 2.787 | 3.231 | 110.5 |
| **3** | F1…H1A–C1A | 2.598 | 3.443 | 151.4 |
| **4** | F1C…H3F–C3D | 2.550 | 3.416 | 151.1 |

## 3. Results and discussion

### 3.1. Description of the molecular structures of complexes **1**–**4**.

#### 3.1.1. Description of the structure of complex **1**

In our previous papers [35,36], we have obtained a dinuclear $Ho^{3+}$ complex with (E)-3-(3- hydroxyl-phenyl)-acrylic acid ligand (L) [36]. The structure of the dinuclear $[Ho(L)_3–(CH_3OH)_2]_2$ shows that it has two methanol molecules in the axial position, which may be replaced by any other bridge ligand. So when N-containing ligand 1,10-phenanthroline as a second ligand was added to similar reaction systems (where transition metal ion $Mn^{2+}$ instead of the $Ho^{3+}$ ion was used), trinuclear $Mn^{2+}$ complex **1** was obtained. Although the three Mn(II) ions in complex **1** are six-coordinated, there are two different Mn(II) ions with different coordination environments (Fig. 1). Mn(1) is six-coordinated with a distorted octahedron geometry formed by four oxygen atoms from three different carboxylato ligands and two nitrogen atoms from the second ligand 1,10-phenanthroline. Mn(2) is also six-coordinated with an octahedron geometry formed by six oxygen atoms from six different carboxylato ligands. In this trinuclear complex, there are six carboxylato ligands (*L1*) that coordinate to three Mn (II) ions, and four of the *L1* ligands coordinate to Mn(II) ions in an $\eta^2$–O bridging mode in a *syn–syn* configuration (C(18)–O(3)–Mn(1) 129.3(2)°; C(18)–O(4–Mn(2) 144.3(2)°). The other two are in a $\eta^3$–O bridge mode. The distance between the two adjacent Mn(II) ions is 3.6381 Å (Table 2). The bond lengths of Mn(II)–O are ranged in 2.093(2)–2.287(2)Å. The bond length of Mn(II)–N is 2.268(3)Å (Table 2).

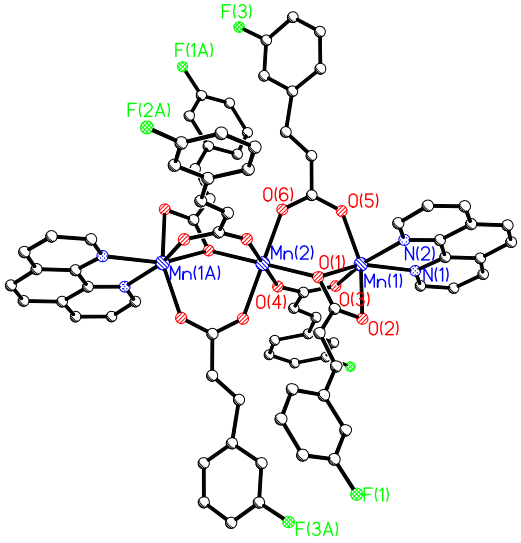


**Fig. 1.** The molecular structure of complex **1**. Hydrogen atoms have been omitted for clarity.

### 3.1.2. Description of the structure of complex **2**

In complex **2**, each Zn(II) is five-coordinated with a square pyramid geometry formed by four oxygen atoms from four different carboxylato ligands *L1* and one nitrogen atom from the bridge ligand 4,4′-bipy (Fig. 2). Carboxylato oxygen in ligand *L1* has only one coordination mode: bis-monodentate ($\eta^2$–O) bridge. Four ligands connect with two zinc atoms to form a paddle-wheel dinuclear complex, which can act as a secondary building unit (SBU). There are potential replaced sites in a paddle-wheel generally. Proceeding from the same design strategy with complex **1**, when bridge ligand 4, 4′-bipy was added to a similar reaction system, paddle-wheel dinuclear complexes are linked to form a one-dimensional chain complex **2**. The $\eta^2$–O bridge mode of carboxylato ligand in complex **2** is in a *syn–syn* configuration (C(9)–O(1)–Zn(1) 126.50(15)°; C(9)–O(2)–Zn(1) (symmetry code: $-x+2$, $-y+1$, $-z+1$) 127.38(16)°). The distance between the Zn(II) ions is 2.9314 Å (Table 3), which is a little longer than the Zn–Zn separation reported previously [38–40]. The bond lengths of Zn(II)–O are ranged in 2.0219(17)–2.2039(17) Å. The bond length of Zn(II)–N is 2.0389(19) Å (Table 3).

### 3.1.3. Description of the structures of complexes **3** and **4**

The structures of **3** and **4** are isomorphous. In our previous work [35,36], we have reported the rare earth metals complexes with (E)-3-(2, or 3, or 4-hydroxyl-phenyl)-acrylic acid ligands exhibiting dinuclear or 1D chain structures. But when transition metals coordinated to (E)-3-(3-fluoro-phenyl)-acrylic acid ligand, a two-dimensional, rectangular grid-like polymeric structure (for compounds **3** and **4**) was resulted. The 2D structure of complex **3** is shown in Fig. 3 together with the coordination environment picture of Mn(II). Selected bond distances and bond angles are listed in Table 4. In the structure of **3**, each Mn(II) is six-coordinated with an elongated octahedron geometry formed by six oxygen atoms from four different carboxylato ligands *L1* and two water molecules. Carboxylato oxygen in ligand *L1* has only one coordination mode: the bis-monodentato ($\eta^2$–O) bridge that coordinate to Mn atoms with an *anti-anti* coordination mode (C(9)–O(1)–Mn(1) 128.08(16)°; C(9) (symmetry code: $x$, $-y+1/2$, $z-1/2$)–O(2)–Mn(1) 131.91(18)°) form a two-dimensional, grid-like polymeric structure. The axial sites are occupied by two water molecules with the Mn–O bond distance of 2.2039(19) Å. The Mn–O bond distances in equatorial plane for the two molecules are 2.1633(19) and 2.1766(19)Å. So the coordination geometry of Mn(II) is an elongated octahedron. The distance between two adjacent Mn(II) ions bridged by carboxylato ligand is 4.9289 Å. There is no solvent molecule occupying the 2D grid (Fig. 3b). If we take the bridging ligand as a line, the two-dimensional grid can also be viewed as a framework consisting of an octahedron (Fig. 3b).

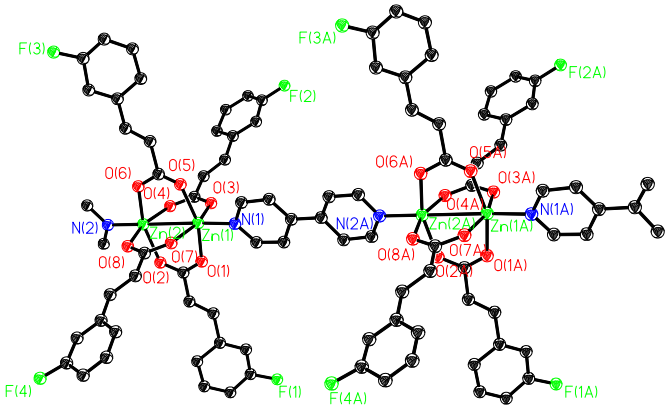


**Fig. 2.** The molecular structure of complex **2**. Hydrogen atoms have been omitted for clarity.

### 3.2. Halogen–hydrogen bonding and halogen–halogen contact in complexes **1–4**.

The intermolecular interaction is one of the most essential issues of supramolecular chemistry. Halogen–halogen bonding is one of the intermolecular interactions that determines the self-assembly of molecules and ions in crystals. However, the study of halogen–hydrogen bonding and halogen–halogen bonding in supramolecular systems has been aroused attention very recently. It is difficult to develop effective supramolecular synthetic strategies that comprise hydrogen–halogen or halogen–halogen bonds. I-containing halogen bonds have been employed in supramolecular chemistry in most cases [41,42], because experimental data confirm the theoretical predictions that the strength of the halogen–halogen bond increases in the order Cl < Br < I [43,44]. Many other kinds of $X\cdots X$ ($X$=Cl, Br, I) and $X\cdots Y$ ($X$=Cl, Br, I; $Y$=O, N, P) contacts were also reported successively [3,18–21]. The nature of halogen–halogen bonding interaction is essentially electrostatic. Halogen atoms function as electron-deficient sites when they form contacts at the pole (electrophilic end), but can also function as electron-rich sites on forming contacts at the equator (nucleophilic end) [45,46]. Theoretical studies predict, and experimental studies confirm that the intermolecular $X\cdots X$ ($X$=Cl, Br, I) interactions may present when the distances of $X\cdots X$ ($X$=Cl, Br, I) are in the range of the sum of van der Waals radii of the two halogen atoms. Recent statistical approaches have shown that halogen atom ($X$) can be characterized by two effective radii: the

**Table 6**
The van der Waals radii of halogen atoms gived by Bondi ($r_B$) and the range of distance ($d$ ($X\cdots X$)) that may exist in halogen–halogen bonding.

| Group | F…F | Cl…Cl | Br…Br | I…I |
|---|---|---|---|---|
| $r_B$ (Å) | 1.47 | 1.75 | 1.85 | 1.98 |
| $d$ ($X\cdots X$) (Å) | 2.74–2.94 | 3.36–3.56 | 3.38–3.68 | 3.89–4.26 |

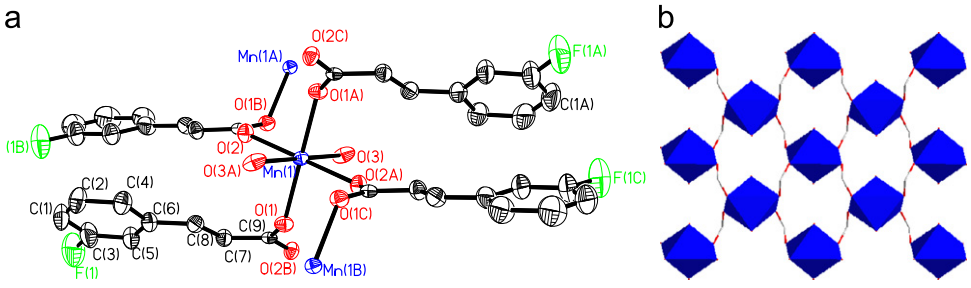


**Fig. 3.** The structure of complex **3**: (a) coordination environments of Mn(II) and (b) octahedron framework viewed down from an axis. Hydrogen atoms have been omitted for clarity.

shortest one ($r_{min}$) in the prolongation of the C–*X* bond and the longer one ($r_{max}$), close to Pauling/Bondi values, perpendicular to the C–*X* bond. As a consequence, the *X*…*X* distance in a C–*X*…*X*–C interaction will be compared to the sum of [$r_{max}(X)$ +$r_{max}(X)$] for a type I interaction, while the contact distance in the type II geometry will be [$r_{min}(X)$+$r_{max}(X)$] [47]. The van der Waals radii of halogen atoms given by Bondi ($r_B$) and the range of distance ($d(X…X)$) which may exist in halogen–halogen bonding are listed in Table 6 [47]. Experimental results prove that it is possible to carefully tune the strength of the halogen bond in a given halocarbon by modifying the substitute on the carbon skeleton [48,49]. However, to the best of our knowledge, there is only one paper about F…F interactions in coordination complex systems reported. One kind of C–F…F–C (2.739 Å) and a series fluorine… fluorine interactions have been observed in complexes obtained from Cu(hfacac)$_2$ (hfacac=hexafluoroacetylacetonate) and dipyrrinato-based ligands (F…F range of 2.8–3.6 Å) [50]. The fluorophenyl-acrylic acid (E)-3-(3–fluoro-phenyl)-acrylic acid (*HL1*) is another resource for halogen–hydrogen bonding with coordinated methanol or water molecules and hydrogen atoms of other ligands, and probably taken for investigation of halogen–halogen interactions. The types of hydrogen bonding and halogen interactions in the crystal lattice of complexes **1**–**4** are C–H…F and C–F…F–C, respectively (Fig. 4).

Two different kinds of C–F…F–C interactions in complexes **1** and **2** can be observed in Fig. 4. Among them, the shortest F…F distance of 2.953 Å was found in the trinuclear complex **1**. This distance (2.953 Å) is very close to the sum of van der Waals radii of F atoms (2.94 Å). The C–F2…F2B angle of 79.1° is equal to the F2…F2B–C angle; this arrangement belongs to the preferred arrangement (Type I, Scheme 1), and the F…F distance in a C–F…F–C interaction should be compared to the sum of [$r_{max}$(F)+$r_{max}$(F)]. By inspiration of the above theory and the distance between Cl…Cl (3.45 Å), Br…Br (3.618 Å) and I…I (3.944 Å) reported in literature [21–23], we proposed that F…F bonding interactions may exist between the trinuclear complex **1**. This crystal structure strongly indicates that the C–F…F–C intermolecular interactions play an important role in the stability of the crystal. The distance of F…F is 3.002 Å in complex **2**, which is slightly longer than the sum of van der Waals radii of F atoms. The C10–F1…F4B and F1…F4B–C13B angles are 96.9° and 127.9°, respectively. These two packing patterns exist in complexes **1** and **2**; the C–F…F–C contacts complement the role of the C–H…F hydrogen bonds in determining the supramolecular structure of these crystalline materials.

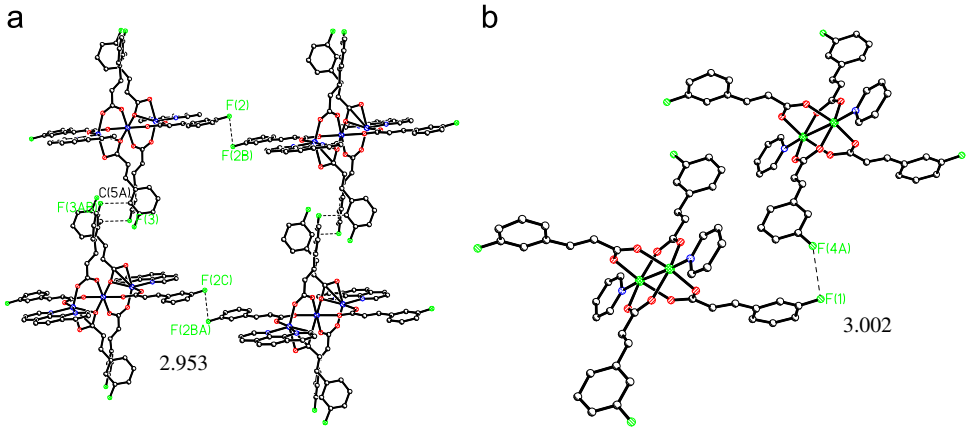


**Fig. 4.** F…F contacts in **2** (a) and **3** (b).

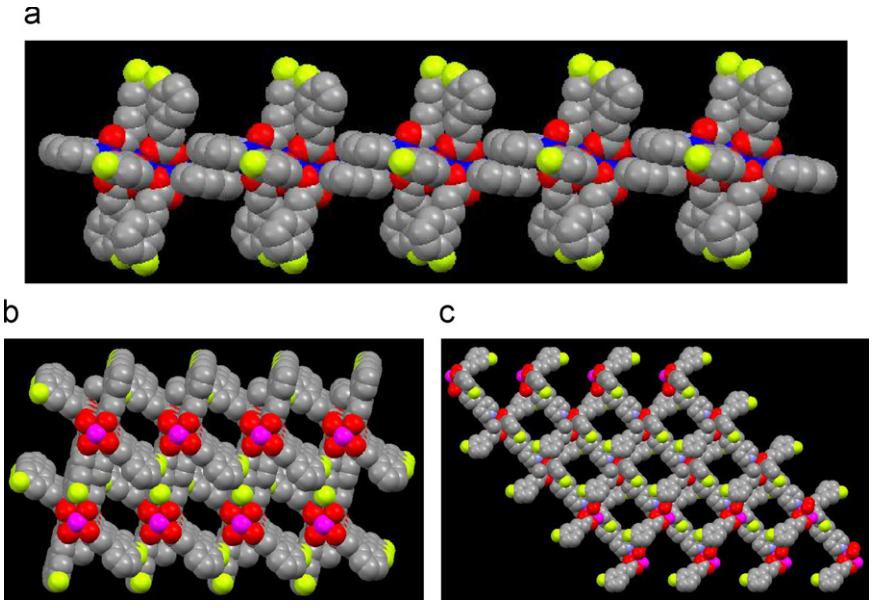


**Fig. 5.** Space-fill pictures of (a) 1D complex **1**, (b) and (c) 3D complex **2** viewed down from *b*+30° and *c*-axis, respectively. Color scheme: C, gray; F, yellow; Mn, blue; Zn, pink; and O, red. (For interpretation of the references to color in this figure legend, the reader is referred to the web version of this article.)

A series of non-conventional C–H…F hydrogen bonds exist in complexes **1**–**4** (Table 5). In addition, the strong *n*–*n* stacking interactions also exist in complex **1** except for the C–H…F hydrogen bonds. The distance between two π–π stacking benzene planes is 3.311 Å, and the one-dimensional chain structure formed through the π–π stacking interactions (Fig. 5a). The complex is further assembled into a 3D ordered structure through non-conventional C–H…F hydrogen bonds interactions and intermolecular electrostatic interactions (Fig. 6a). In complex **2**, we noted that the one-dimensional coordination chains connect with each other via non-conventional H-bonding interactions: F1…H12B–C12A: 2.787 Å, 3.231 Å, 110.5° to form a 2D layer structure. These layers are then aggregated into the final three-dimensional non-interpenetration lattice via C–F…F–C contacts (Fig. 6b). There are also one-dimensional channels in 3D complex **2** viewed down from different directions (Fig. 5a and b). Complexes **3** and **4** that have 2D grid like structure are all further assembled into 3D ordered organic–inorganic hybrid layer structure through C–H…F hydrogen bonds interactions (Fig. 6c and d).

### 3.3. Magnetic properties

The magnetic properties of complexes **3** and **4** were investigated in the 2.0–300.0 K range at 2000 Oe. The magnetic properties of complexes **3** and **4** in the form of $\chi_m T$ vs. $T$ and $\chi_m^{-1}$ vs. $T$ plots ($\chi_m$ is the molar susceptibility per two Mn(II) or Co(II) ions) are shown in Fig. 7a and 7b, respectively. At 300 K, the $\chi_m T$ values are 4.73 and 2.85 emu K mol$^{-1}$ for **3** and **4**, respectively. These values are slightly larger than the theoretical value when there is no magnetic interaction for **3** (4.375 emu K mol$^{-1}$, $S=5/2$, $g=2.0$), and smaller for **4** (2.93 emu K mol$^{-1}$, $S=3/2$, $g=2.5$). The larger experimental value of complex **3** than the corresponding spin only value can be assigned to

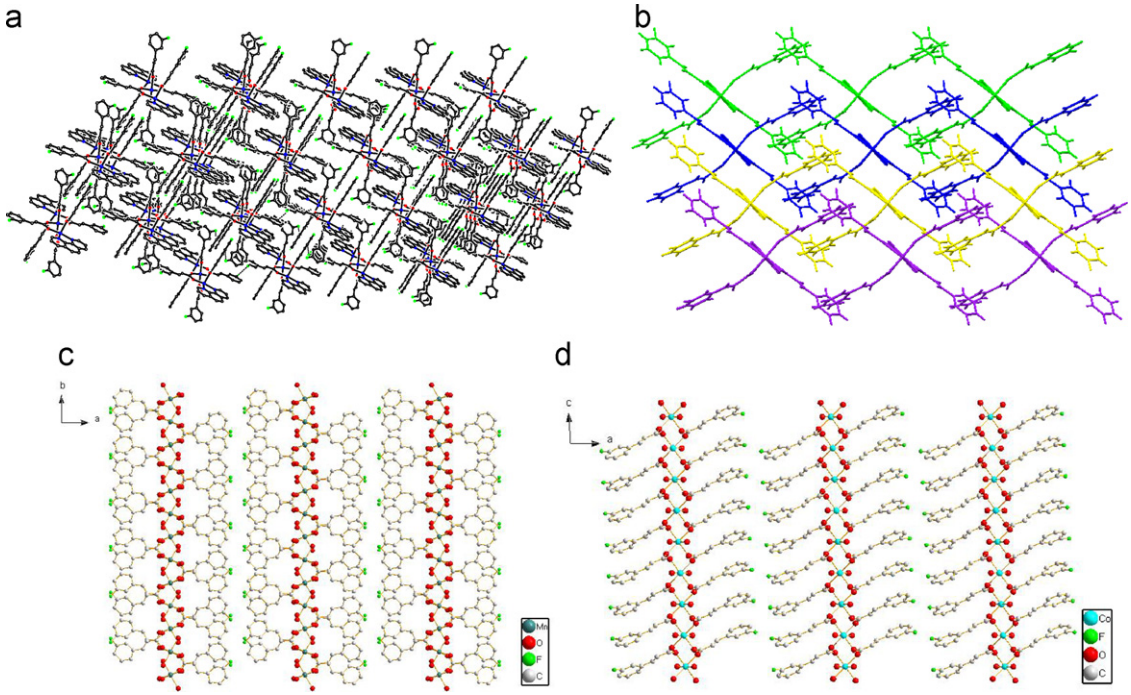


**Fig. 6.** 3D packing pictures of **1** (a), **2** (b), **3** (c) and **4** (d) viewed from *a*, *b*+30°, *c* and *b* axes, respectively.

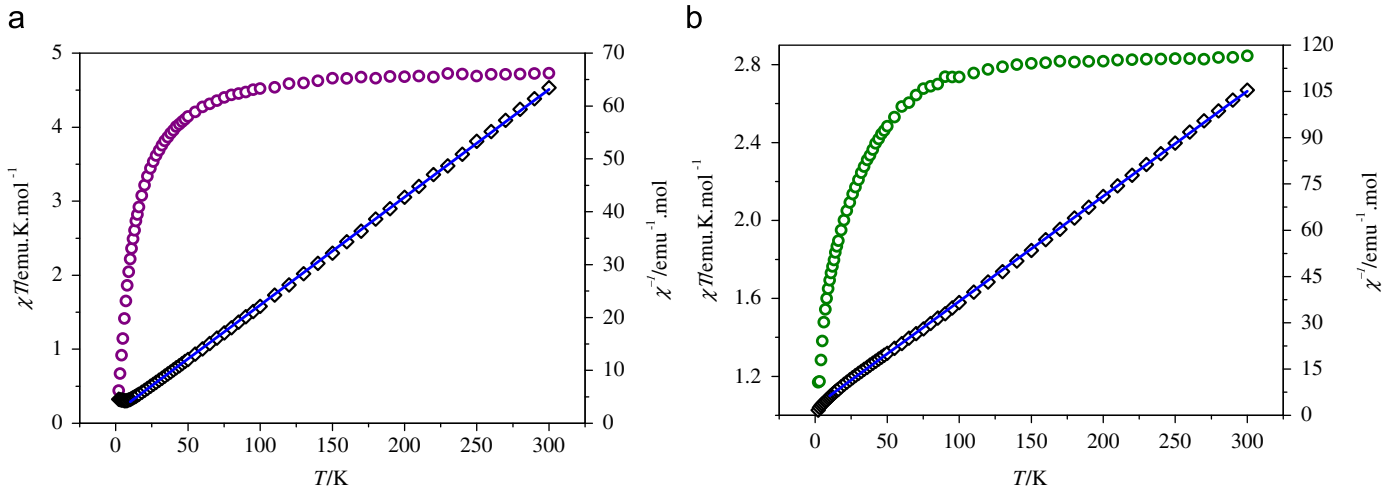


**Fig. 7.** Plots of $\chi_m T$ and $\chi_m^{-1}$ vs. $T$ of **3** (a) and **4** (b).

the unquenched orbital-moment as a result of spin–orbit coupling in the distorted octahedral coordinated Mn(II) ions, and lower $\chi_m T$ values of complex **4** than the spin-only value are expected for a magnetically isolated high-spin Co(II) ion [51–54]. On cooling, the $\chi_m T$ values decrease gradually in the temperature range 300–50 K and then abruptly below 50 K for **3** and 100 K for **4**. This behavior indicates the presence of overall weak antiferromagnetic exchange interactions between the Mn(II) ions and between the Co(II) ions in **3** and **4**, respectively. Over the range of 10–300 K, the magnetic data are consistent with the Curie–Weiss law, with the Curie constant and the $\theta$ value being 4.91 emu K mol$^{-1}$, −9.77 K and 2.94 emu K mol$^{-1}$, −8.53 K for **3** and **4**, respectively. The negative $\theta$ value and decreasing tendency of $\chi_m T$ in the high temperature region should arise from antiferromagnetic exchange coupling, but also reflect the single ion spin–orbit coupling for the isolated Co(II) ion possessing an octahedral ligand field [51].

As described in the structural section, compounds **3** and **4** are isomorphous and their structures can be described as a two-dimensional net in which the carboxylato bridges link the metal ions in an *anti-anti* mode. It has been reported that the strong antiferromagnetic interactions are mediated by the *anti-anti* bridging modes [55–57], whereas either weak ferromagnetic or weak antiferromagnetic interactions occur in the *syn–anti* and *syn–syn* carboxylato bridged copper(II) complexes [56,58,59]. Herein, we found that the magnetic properties of carboxylato bridged manganese(II) and cobalt(II) complexes are also in line with this view. However, the study of the magnetic properties of carboxylato bridged manganese(II) and cobalt(II) complexes are very perplexing. The weak antiferromagnetic and strong ferromagnetic interactions can both be mediated by the *syn–syn* bridging modes and either ferro- or antiferromagnetic interactions through the *anti–anti* [60] and *anti–syn* [61] conformations occur in cobalt(II) complexes [62,63]; and the *syn–syn* or *syn–anti* carboxylato bridge always induces antiferromagnetic coupling between manganese(II) ions, as has been observed in a number of compounds with single or double carboxylato bridges [52,64–69].

## 4. Conclusions

Using (E)-3-(3–fluoro-phenyl)-acrylic acid as the primary ligands, a series of trinuclear, 1D and 2D coordination complexes have been prepared based on the molecular design via structural tuning of the second ligand. The present study demonstrates a facile method for the synthesis of different dimension complexes of the same ligand. In 3D well-defined structures, C–F…F–C interactions combining with non-conventional H-bonding and π–π stacking play an important role in the self-assembly of these pre-designed simple complexes. In this work, the short F…F contact with the distance of 2.953 Å in complex **1** was discovered. These results are important for the further study of supramolecular complex involving halogen–halogen interactions. We hope that this result can produce the effect of "use a little to gain a big". Further studies are ongoing.

## Acknowledgments

We thank the National Science Council of the People's Republic of China for supporting this research (Nos. 20571011 and 20771014) and also the specialized research fund for the doctoral program of higher education, State Education Ministry of China (20091101110038) and the 111 Project B07012 in China.

## References

[1] L. Brammer, G. Espallargas, S. Libri, Cryst. Eng. Commun. 10 (2008) 1712–1737.
[2] P. Metrangolo, F. Meyer, T. Pilati, G. Resnati, G. Terraneo, Angew. Chem. Int. Ed. 47 (2008) 6114–6127.
[3] M. Fourmigue, Curr. Opin., Solid State Mater. Sci. 13 (2009) 36–45.
[4] C.S. Liu, P.Q. Chen, E.C. Yang, et al., Inorg. Chem. 45 (2006) 5812–5821.
[5] J.J. Wang, C.S. Liu, T.L. Hu, et al., Cryst. Eng. Commun. 10 (2008) 681–692.
[6] J. Luo, T. Lei, L. Wang, et al., J. Am. Chem. Soc. 131 (2009) 2076–2077.
[7] A.T. Cate, H. Kooijman, A.L. Spek, et al., J. Am. Chem. Soc. 126 (2004) 3801–3808.
[8] C.B. Aakery, A.M. Beatty, B.A. Helfrich, J. Am. Chem. Soc. 124 (2002) 14425–14432.
[9] S. Derossi, L. Brammer, C.A. Hunter, et al., Inorg. Chem. 48 (2009) 1666–1677.
[10] Y.B. Men, J.L. Sun, Z.T. Huang, et al., Angew. Chem. Int. Ed. 48 (2009) 1–5.
[11] K. Chadwick, G. Sadiq, R.J. Davey, et al., Cryst. Growth Des. 9 (2009) 1278–1279.
[12] L. Rajput, K. Biradha, Cryst. Growth Des. 9 (2009) 40–42.
[13] T.R. Shattock, K.K. Arora, P. Vishweshwar, et al., Cryst. Growth Des. 8 (2008) 4533–4545.
[14] L.S. Reddy, A. Nangia, V.M. Lynch, Cryst. Growth Des. 4 (2004) 89–94.
[15] A.V. Puga, F Teixidor, R. Sillanp, et al., Chem. Eur. J. 15 (2009) 9764–9772.
[16] M.E. Guillermo, B. Lee, R.A. David, et al., J. Am. Chem. Soc. 130 (2008) 9058–9071.
[17] A. Kovacs, Z. Varga, Coord. Chem. Rev. 250 (2006) 710–727.
[18] F.F. Awwadi, R.D. Willett, K.A. Peterson, B. Twamley, Chem. Eur. J. 12 (2006) 8952–8960.
[19] G.R. Desiraju, R. Parthasarathy, J. Am. Chem. Soc. 111 (1989) 8725–8726.
[20] B. Christer, Aakeroy, J. Am. Chem. Soc. 129 (2007) 13772–13773.
[21] D. Cincic, W. Jones, J. Am. Chem. Soc. 130 (2008) 7524–7525.
[22] A. Firas, F. Salim, R.D. Haddad, et al., Cryst. Growth Des. 10 (2010) 158–164.
[23] K. Yuka, M. Jin, A. Tetsuo, et al., Cryst. Growth Des. 10 (2010) 685–690.
[24] J.J. Wolff, et al., Chem. Eur. J. 5 (1999) 29–38.
[25] D. Chopra, T.S. Cameron, J.D. Ferrara, et al., J. Phys. Chem. A 110 (2006) 10465–10477.
[26] A. Bach, D. Lentz, P. Luger, J. Phys. Chem. A 105 (2001) 7405–7412.
[27] G. Asensio, M.M. Simon, P. Aleman, et al., Cryst. Growth Des. 6 (2006) 2769–2778.
[28] A.R. Choudhury, T.N.G. Row, Cryst. Growth Des. 4 (2004) 47–52.
[29] A.R. Choudhury, T.N.G. Row, Cryst. Eng. Commun. 8 (2006) 265–274.
[30] N. Oshrit, B. Joel, K. Vladimir, Angew. Chem. Int. Ed. 36 (1997) 601–603.
[31] M. Pierangelo, P. Tullio, S. Andrea, et al., Curr. Opin. Colloid and Interface Sci. 8 (2003) 215–222.
[32] R. Bertani, P. Sgarbossa, A. Venzo, et al., Coord. Chem. Rev. 254 (2010) 677–695.
[33] B. Roberta, C. Fanny, G. Mario, et al., Inorg. Chim. Acta 360 (2007) 1191–1199.
[34] B. Deepak, B.G. Salunke, R.G. Hazra, et al., J. Mol. Struct. 892 (2008) 246–253.
[35] H. Li., C.W. Hu, J. Solid State Chem. 177 (2004) 4501–4507.
[36] H. Li, C.W. Hu, J. Mol. Struct. 743 (2005) 97–101.
[37] G.M. Sheldrick, Shelxtl97, University of Göttingen, Germany, 1997.
[38] E. Carmona, A. Galindo, Angew. Chem. Int. Ed. 47 (2008) 6526–6536.
[39] Z.L. Zhu, R.J. Wright, M.M. Olmstead, et al., Angew. Chem. Int. Ed. 45 (2006) 5807–5810.
[40] X.J. Yang, J. Yu, Y. Liu, et al., Chem. Commun. 13 (2007) 2363–2365.
[41] R.B. Walsh, C.W. Padgett, P. Metrangolo, G. Resnati, T.W. Hanks, W.T. Pennington, Cryst. Growth Des. 1 (2001) 165–175.
[42] E. Corradi, S.V. Meille, M.T. Messina, P. Metrangolo, G. Resnati, Angew. Chem. Int. Ed. 39 (2000) 1782–1786.
[43] M. Fourmigue, P. Batail, Chem. Rev. 104 (2004) 5379–5418.
[44] P. Metrangolo, G. Resnati, et al., Angew. Chem. Int. Ed. 47 (2008) 6114–6127.
[45] Y.X. Lu, J.W. Zou, Y.H. Wang, et al., Theochem 766 (2006) 119–124.
[46] H.G. Loehr, A. Engel, H.P. Josel, et al., J. Org. Chem. 49 (1984) 1621–1627.
[47] S.C. Nyburg, C.H. Faerman, Acta Crystallogr. B 41 (1985) 274–279.
[48] G. Valerio, G. Raos, S.V. Meille, P. Metrangolo, G. Resnati, J. Phys. Chem. A 104 (2000) 1617–1620.
[49] R Weiss, O. Schwab, F. Hampel, Chem. Eur. J. 5 (1999) 968–974.
[50] J. Granifo, D. Toledo, M.T. Garland, R. Baggio, J. Fluorine Chem. 131 (2010) 510–516.
[51] H.L. Wang, D.P. Zhang, D.F. Sun, et al., Cryst. Growth Des. 9 (2009) 5273–5282.
[52] Y.Q. Wang, Q.X. Jia, E.Q. Gao, Inorg. Chem. 49 (2010) 1551–1660.
[53] Z. Chen, Y. Li, Y. Song, Dalton Trans. 27 (2009) 5290–5299.
[54] F.P. Huang, J.L. Tian, P. Cheng, et al., Cryst. Growth Des. 10 (2010) 1145–1154.
[55] J. Pasań, J. Sanchiz, C. Ruiz-Pérez, F. Lloret, M. Julve, Inorg. Chem. 44 (2005) 7794–7801.
[56] R. Baldoma, M. Monfort, J. Ribas, X. Solans, M.A. Maestro, Inorg. Chem. 45 (2006) 8144–8155.
[57] A.K. Ghosh, D. Ghoshal, E. Zangrando, J. Ribas, N.R. Chaudhuri, Inorg. Chem. 46 (2007) 3057–3071.
[58] C. Ruiz-Pérez, J. Sanchiz, M.H. Molina, F. Lloret, M. Julve, Inorg. Chem. 39 (2000) 1363–1370.
[59] F.S. Delgado, J. Sanchiz, C. Ruiz-Pérez, F. Lloret, M. Julve, Inorg. Chem. 42 (2003) 5938–5948.
[60] J.M. Rueff, N. Masciocchi, P. Rabu, et al., Eur. J. Inorg. Chem. 11 (2001) 2843–2848.
[61] F.S. Delgado, M. Hernandez-Molina, J. Sanchiz, et al., Cryst. Eng. Commun. 6 (2004) 106–111.
[62] H.P. Jia, W. Li, Z.F. Zhu, et al., Eur. J. Inorg. Chem. 21 (2006) 4264–4270.
[63] O. Fabelo, L.C. Delgado, J. Pasan, Inorg. Chem. 48 (2009) 11342–11351.
[64] W. Li, H.P. Jia, Z.F. Ju, J. Zhang, Dalton Trans. 39 (2008) 5350–5357.
[65] L. Lecren, O. Roubeau, Y.G. Li, Dalton Trans. 6 (2008) 755–766.
[66] C.M. Liu, D.Q. Zhang, D.B. Zhu, Inorg. Chem. 48 (2009) 4980–4987.
[67] W. Chen, Q. Yue, C. Chen, et al., Dalton Trans. 1 (2003) 28–30.
[68] M.H. Zeng, M.C. Wu, X.M. Chen, Inorg. Chem. 46 (2007) 7241–7243.
[69] Y.L. Zhou, M.C. Wu, H. Liang, Inorg. Chem. 48 (2009) 10146–10150.